Polymorphism, Phase Transformations, and Oxide Ion Conductivity in $Bi_{1.56}U_{0.22}La_{0.22}O_{3.33}$

J. M. Amarilla, R. M. Rojas,* and J. M. Rojo

Instituto de Ciencia de Materiales de Madrid, Consejo Superior de Investigaciones Científicas, Cantoblanco, 28049 Madrid, Spain

Received August 18, 1997. Revised Manuscript Received November 4, 1997

This paper deals with the polymorphism, phase transitions, and the oxide ion conduction of $Bi_{1.56}U_{0.22}La_{0.22}O_{3.33}$. Thermal treatment at 950 °C of a mixture of α-Bi_2O_3 and $LaUO_{4+x}$, followed by slow cooling to room-temperature, yields a hexagonal phase of that composition with cell parameters $a_H = 4.0066(7)$ and $c_H = 9.543(2)$ Å. Quenching of the reaction mixture from 950 °C leads to the formation of a cubic fluorite-type phase with $a_c = 5.6273(8)$ Å. Annealing of both cubic and hexagonal phases at 600 °C for 500 h yields a new polymorph that is indexed with a monoclinic lattice, the cell parameters being $a_M = 7.778(3)$, $b_M = 7.834(4)$, $c_M = 5.763(3)$ Å, and $\beta = 89.71(2)°$. Phase transitions experienced by each polymorph with temperature are followed by high-temperature X-ray powder diffraction. The three phases are transformed into a new C* cubic phase at temperatures above 820 °C. The oxide ion conduction exhibited by each $Bi_{1.56}U_{0.22}La_{0.22}O_{3.33}$ polymorph is rather different. At 300 °C the cubic phase, which is the best conducting one, shows a value of $\sigma = 7.2 \times 10^{-5}$ S cm^{-1}, the conductivity of the hexagonal phase is 2.5×10^{-5} S cm^{-1}, and the monoclinic phase shows the lowest conductivity, 6.6×10^{-7} S cm^{-1}. The plot of conductivity vs inverse temperature shows a linear dependence for each phase. The nonlinear dependencies also observed in the conductivity plots are related to structural transformations taking place during thermal treatments.

Introduction

It is well-known that the high-temperature modification of bismuth sesquioxide (δ-Bi_2O_3) is the best solid-state oxide ion conductor, the conductivity being about 2 orders of magnitude higher than that of conventional oxide conductors such as stabilized zirconia.[1] The cubic δ-phase is stable between 728 °C and the melting point at 824 °C, although stabilization at room temperature of that phase can be attained by addition of several oxides.[1−4] This fact is the reason why materials based on bismuth sesquioxide are very promising as solid electrolytes in electrochemical devices such as solid oxide fuel cells (SOFCs)[3] and oxygen pumps.[5] However, the ionic conductivity of δ-Bi_2O_3 decreases by doping,[6] and the conductivity of Bi_2O_3-based materials is strongly dependent on the dopant cation used as well as on composition and structural characteristics.[1,3,7−9] It has also been shown that many of the stabilized δ-phases are quenched high-temperature phases, and by annealing they are transformed into less conductive low-temperature stable phases.[10,11] All these particular aspects have a great influence on the performance of the Bi_2O_3-based materials as solid electrolytes in electrochemical devices.

In a previous paper[12] we have reported on the synthesis of the new bismuth-based oxide materials of general formula $Bi_{2-2x}U_xLa_xO_{3+3x/2}$ ($0.038 \le x \le 0.333$). The long-term thermal stability of these oxides was studied by annealing the materials at 600 °C for either short (50 h) or long (>500 h) periods. The hexagonal phase at $x = 0.333$ ($Bi_{1.33}U_{0.33}La_{0.33}O_{3.5}$) was the only phase that did not show structural modifications after treatments longer than 1700 h at 600 °C. The hexagonal and cubic polymorphs at $x = 0.222$ ($Bi_{1.56}U_{0.22}La_{0.22}O_{3.33}$) transformed into another phase, whose X-ray powder pattern was tentatively indexed on the basis of a tetragonal cell with parameters $a_T = 7.806$ and $c_T = 5.768$ Å,[12] very close to those shown by the tetragonal β-Bi_2O_3 phase.[13] Annealing of all the other compositions yielded mixtures of the "tetragonal" $x = 0.222$ polymorph and/or the corresponding hexagonal phase and/or α-Bi_2O_3.[12]

We have considered it worthwhile to study in detail the polymorphism and ion conduction properties of the

(1) Takahashi, T. Iwahara, H. *Mater. Res. Bull.* **1978**, *13*, 1447.
(2) Verkerk, M. J.; Keizer, K.; Burggraaf, A. J. *J. Appl. Electrochem.* **1980**, *10*, 81.
(3) Azad, A. M.; Larose, S.; Akbar, S. A. *J. Mater. Sci.* **1994**, *29*, 4135.
(4) Shuk, P.; Wiemhöfer, H. D.; Guth, U.; Göpel, W.; Greenblatt, M. *Solid State Ionics* **1996**, *89*, 179.
(5) Naumovich, E. N.; Kharton, V. V.; Samokhval, A. V.; Kovalevsky, A. V. *Solid State Ionics* **1997**, *93*, 95.
(6) Burggraaf, A. J.; Boukamp, B. A.; Vinke I. C.; de Vries, K. J. In *Advances in Solid State Chemistry*; Catlow, C. R. A., Ed.; Jai Press: London, 1989; Vol.1, p 259.
(7) Iwahara, H.; Esaka, T.; Sato, T.; Takahashi, T. *J. Solid State Chem.* **1981**, *39*, 173.
(8) Fung, K. Z.; Cheng, J.; Virkar, A. V. *J. Am. Ceram. Soc.* **1993**, *76*, 2403.
(9) Amarilla, J. M.; Rojas, R. M.; Rojo, J. M. *Chem. Mater.* **1997**, *9*, 1262.
(10) Watanabe, A. *Solid State Ionics* **1990**, *40/41*, 889.
(11) Watanabe, A. *Solid State Ionics* **1996**, *86−88*, 1427.
(12) Amarilla, J. M.; Rojas, R. M. *Chem. Mater.* **1996**, *8*, 401.
(13) Blower, S. K.; Greaves, C. *Acta Crystallogr.* **1988**, *C44*, 587.

S0897-4756(97)00573-5 CCC: $15.00
Published on Web 01/07/1998

$Bi_{1.56}U_{0.22}La_{0.22}O_{3.33}$ oxide. The phase transformations experienced by each polymorph with temperature as well as their associated ionic conductivity have been examined. The nonlinear Arrhenius behaviors are also discussed in terms of temperature-dependent structural transformations.

Experimental Section

Both hexagonal (H) and cubic (C) $Bi_{1.56}U_{0.22}La_{0.22}O_{3.33}$ polymorphs were synthesized by heating at 950 °C a stoichiometric mixture of α-Bi_2O_3 and lanthanum uranate, $LaUO_{4+x}$; the latter had been previously obtained by thermal decomposition at 850 °C of the organic precursor lanthanum uranyl propionate, $LaUO_2(C_2H_5COO)_5 \cdot 3H_2O$. A detailed description of the synthesis procedure has been reported elsewhere.[9,12] When the reaction mixture was slowly cooled to room temperature, the hexagonal $Bi_{1.56}U_{0.22}La_{0.22}O_{3.33}$ phase was obtained as a well-crystallized material. The cubic polymorph was synthesized following the same procedure, but after the heat treatment at 950 °C the sample was quenched in air. When both hexagonal and cubic phases are annealed at 600 °C for 500 h, another polymorph, hereafter referred to as M, is obtained.

X-ray powder diffraction patterns were recorded at room temperature with a Siemens D-501 diffractometer, with Cu Kα radiation. The patterns were scanned at 0.02° (2θ) and 5 s/step counting time within the range $4° \leq 2\theta \leq 120°$. In some particular case a Philips X'Pert-MPD diffractometer was used. The powder data from 10° to 60° in 2θ were collected by using strictly monochromatic Cu Kα_1 radiation, at 0.02° (2θ) and 10 s/step counting time. High-temperature X-ray diffraction studies were carried out using an Anton Paar chamber mounted on a Philips PW 1710 diffractometer. The scans were carried out at 2° (2θ) min^{-1} scan rate between $16° < 2\theta < 75°$. The samples were placed on a platinum strip which also acts as the heating element. The temperature was measured by a Pt−13% Rh/Pt thermocouple welded onto the back of the platinum strip. The experiments were carried out in air in the temperature range 25−850 °C. The heating/cooling rate was 2 °C min^{-1}. In some particular cases, the temperature was held for some time, and patterns were then recorded. Cell parameters were refined by using the program CELREF.[14] Differential thermal analysis (DTA) and thermogravimetric (TG) curves were simultaneously recorded on a Stanton STA 781 instrument. A ≈80−100 mg batch of each sample was heated in air at 10 °C min^{-1}; α-Al_2O_3 was used as reference material. Differential scanning calorimetry (DSC) measurements were performed in a Seiko DSC 320U instrument at 10 °C min^{-1} heating/cooling rate. Sintered α-Al_2O_3 was used as reference, and the scans were recorded on ≈90 mg batches of the material which adopted the form of sintered pellets as those used for the electrical measurements. Electrical conductivity measurements were carried out in a 1174 Solartron frequency response analyzer connected to a 1286 Solartron electrochemical interface. Pellets of ≈6 mm diameter and 1 mm thickness were prepared by compaction of the powder sample under pressure of 1500 kg cm^{-2}. Pellets of the hexagonal and cubic polymorph were sintered at 950 °C for 12 h. Platinum electrodes were painted on the two planar surfaces of the sintered pellets with platinum paste (Engelhard 6082); then they were dried at 200 °C for 1 h and fired at 950 °C for 4 h. The pellet of the hexagonal phase was slowly cooled from 950 °C to room temperature (1 °C min^{-1}), and the pellet corresponding to the cubic phase was quenched in air. To avoid phase transitions taking place at $T > 650$ °C, pellets of the M polymorph were sintered at 500 °C for 12 h. Silver electrodes were painted onto the two planar surfaces; then they were dried at 200 °C, sintered at 600 °C for 2 h, and then cooled at 1 °C min^{-1} to room temperature. Before and after the electrical measurements the crystalline phase of each pellet was checked by X-ray powder diffraction. The impedance measurements were carried out in the frequency range $1-10^5$ Hz at different temperatures (190−980 °C) with the pellet in still air. In the heating and cooling runs the increment of temperature was 30 °C, and before each measurement the sample was kept at the indicated temperature for 20 min.

(14) Laugier, J.; Filhol, A. (CELREF), I.L.L. Grenoble, France, unpublished, P. C. version, 1991.

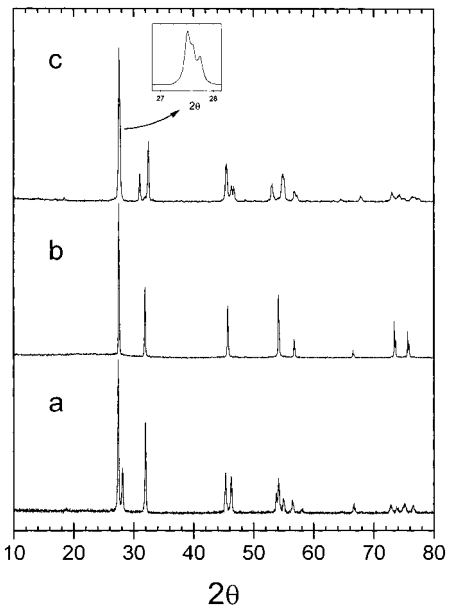

Figure 1. X-ray powder diffraction patterns recorded at room temperature for $Bi_{1.56}U_{0.22}La_{0.22}O_{3.33}$: (a) slowly cooled from 950 °C (hexagonal); (b) quenched from 950 °C (cubic); (c) either (a) or (b) annealed at 600 °C for 500 h (monoclinic). The inset is an enlargement of the 27°−28° 2θ zone.

Results

X-ray Powder Diffraction. The X-ray powder diffraction pattern of the hexagonal $Bi_{1.56}U_{0.22}La_{0.22}O_{3.33}$ polymorph is presented in Figure 1a. All the maxima have been indexed in a hexagonal lattice of cell parameters $a_H = 4.0066(7)$, $c_H = 9.543(2)$ Å, and $V_H = 132.66$ Å^3.[12] When this phase is heated from room temperature to 950 °C and then quenched in air, a face-centered cubic fluorite-type phase (Figure 1b) with lattice parameter $a_C = 5.6273(8)$ Å ($V_C = 178.19$ Å^3) is obtained.[12] Annealing at 600 °C for 500 h of both at room-temperature hexagonal and cubic polymorphs leads to the formation of another polymorph, M, whose X-ray pattern is shown in Figure 1c. Due to the similarity between this pattern and that shown by the tetragonal β-Bi_2O_3,[13] the pattern was tentatively indexed in a tetragonal lattice.[12] However, some diffraction peaks showed an asymmetric profile suggesting some unresolved splitting. When the same pattern is recorded with strictly monochromatic Cu Kα_1 radiation, splitting of those maxima indicating a lower symmetry is clearly observed (see inset in Figure 1c). All the diffraction maxima can be indexed in a monoclinic lattice of parameters $a_M = 7.778(3)$, $b_M = 7.834(4)$, $c_M = 5.763(3)$ Å, $\beta = 89.71(2)°$, and $V = 351.15$ Å^3 (Table 1).

Thermal Analysis. The compositional stability of the three polymorphs with temperature was assessed by thermogravimetric (TG) analysis. The TG curves (not shown) only showed a plateau within the temperature range explored (room temperature to 950 °C), indicating that the samples did not undergo weight

Table 1. X-ray Powder Diffraction Data for Monoclinic $Bi_{1.56}U_{0.22}La_{0.22}O_{3.33}$ (a_M = 7.778(3), b_M = 7.834(4), c_M = 5.763(3) Å, β = 89.71(2)°)

hkl	$2\theta_{exp}$	$2\theta_{cal}$	I/I_0
0 2 1	27.531	27.512	100
2 0 1	27.592	27.583	70
2 0 −1	27.716	27.718	57
0 0 2	31.001	31.012	21
2 2 0	32.428	32.416	46
2 2 2	45.425	45.388	29
0 4 0	46.252	46.322	10
4 0 0	46.691	46.680	11
2 0 3	53.025	53.022	12
2 4 1	54.819	54.764	19
4 2 −1	55.084	55.114	6
0 4 2	56.754	56.792	8
4 0 −2	57.199	57.248	4
5 2 0	64.496	64.396	2
0 1 4	65.881	65.862	1
4 4 0	67.789	67.872	4
2 5 −2	72.965	72.896	6
5 2 −2	73.372	73.348	1
6 1 0	74.051	74.078	4
6 0 1	74.951	74.958	2
3 1 4	76.344	76.376	4

change during the dynamic heat treatments. Figure 2 shows the DSC curves for the hexagonal, cubic, and monoclinic $Bi_{1.56}U_{0.22}La_{0.22}O_{3.33}$ polymorphs in the temperature range where transformations take place (600−850 °C). The DSC heating curve recorded for the hexagonal phase (Figure 2a) shows a very weak endothermic effect in the temperature range 745−825 °C, with the enthalpy of the reaction, deduced from the peak area being 2.40 J g^{-1}. For the cubic fcc-type phase (Figure 2b) two consecutive exo- and endothermic effects are observed between 650 and 820 °C, with enthalpies of −0.91 and 2.42 J g^{-1}, respectively. It is worth noting the small energy involved in these endothermic processes, being ca. half of the values reported for the $\beta \rightleftarrows \gamma$ phase transition in $Bi_4V_2O_{11}$.[15] The DSC heating trace for the monoclinic polymorph (Figure 2c) shows an asymmetric endothermal effect between 690 and 760 °C (T_{max} = 733 °C); the enthalpy associated with the effect (17.71 J g^{-1}) is significantly higher than those measured for the other polymorphs. The DSC cooling curves for the three polymorphs are similar and only show an exothermic effect, which appears between 750 and 660 °C. In Figure 2d, the DSC cooling curve recorded for the hexagonal polymorph is depicted as a representative example. It is worth noting that the enthalpy associated with the exothermic effects on cooling are practically the same than those measured for the hexagonal and cubic polymorphs on heating, ≈−2 J g^{-1}. Some hysteresis in temperature is observed when the endothermic peaks recorded on heating are compared with the exothermic ones taking place on cooling.

Electrical Measurements. The impedance plots (−Z'' vs Z') of the cubic, hexagonal, and monoclinic polymorphs obtained at 220 °C are shown in Figure 3a, b, and c, respectively. The plot of the cubic phase at 700 °C is shown in Figure 3d. At low temperature only one arc is observed for the three polymorphs. However, when the pellets are heated at higher temperatures, this arc disappears and a new arc is developed. The new arc, which shows a capacitance of 0.1−1 mF for the three pellets, is ascribed to electrode reactions.[16] The former arc shows a capacitance in the range 10−20 pF,

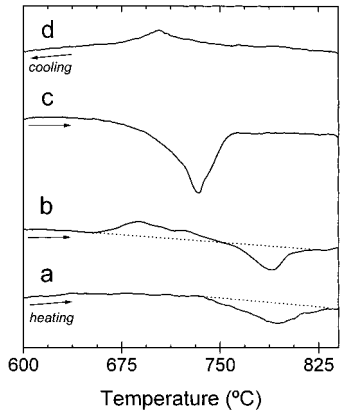

Figure 2. DSC heating curves recorded for (a) hexagonal, (b) cubic, (c) monoclinic $Bi_{1.56}U_{0.22}La_{0.22}O_{3.33}$ polymorphs, and (d) DSC cooling curve for the hexagonal polymorph. Only the temperature range where transformations occur is presented.

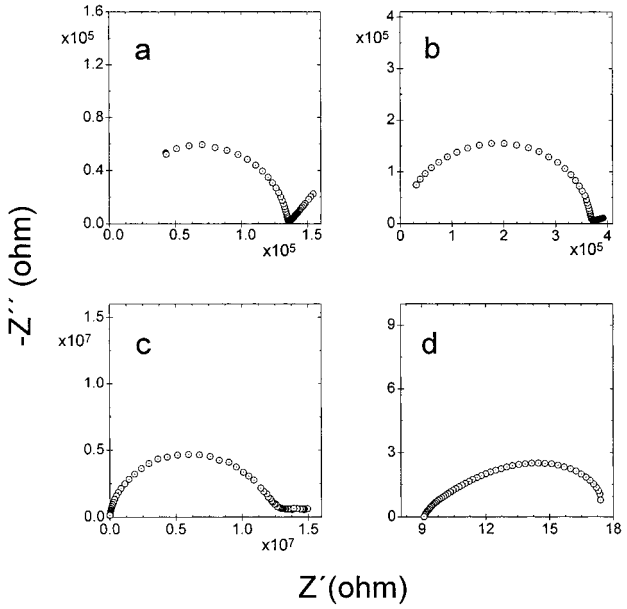

Figure 3. Impedance plots (imaginary vs real part) recorded at 220 °C for the (a) cubic, (b) hexagonal; (c) monoclinic $Bi_{1.56}U_{0.22}La_{0.22}O_{3.33}$ polymorphs, and (d) cubic polymorph at 700 °C.

which is the order of magnitude usually found for grain-interior response.[17] The resistance of the pellets at each temperature is determined by intersection of this arc with the real axis, and then the value of dc conductivity is calculated as usual.

To ascertain whether the impedance arc observed at low temperature is also affected by grain-boundary response, i.e., by movement of O^{2-} ions through the boundary of neighbor grains, we have calculated the imaginary part of the electric modulus (M'') and analyzed the variation of this parameter as a function of frequency and temperature. M'' is chosen because it gives information on grain-interior response and is not usually affected by grain-boundary and electrode ef-

(15) Joubert, O.; Jouanneaux, A.; Ganne, M. *Mater. Res. Bull.* **1994**, *29*, 175.
(16) Ross MacDonald, J.; Johnson, W. B. In *Impedance Spectroscopy*; Ross MacDonald, J., Ed.; John Wiley and Sons: New York, 1987; Chapter 1.
(17) Irvin, J. T. S.; Sinclair, D. C.; West, A. R. *Adv. Mater.* **1990**, *2*, 132.

Table 2. Activation Energy (E), Preexponential Factor (log σ_0), and Conductivity (σ) Associated with Phases Detected at the Temperatures Indicated during the Thermal Treatments of the Hexagonal, Cubic, and Monoclinic $Bi_{1.56}U_{0.22}La_{0.22}O_{3.33}$ Polymorphs

polymorph	T (°C) range	$E\sigma$ (eV)	log σ_0 (S cm^{-1})	$\sigma_{300°C}$ (S cm^{-1})	E_f (eV)	log f_0 (Hz)
cubic	220−340	0.91(2)	3.94(2)	7.2E−5[a]	0.90(2)	12.8(2)
cubic (C*) from cubic	820−970	0.47(3)	1.5(2)	*b*		
hexagonal from cubic	460−220	0.90(1)	3.37(2)	2.7E−5	0.87(2)	13.4(2)
hexagonal	220−460	0.91(1)	3.35(2)	2.5E−5	0.87(2)	13.7(2)
cubic (C*) from hexagonal	820−970	0.50(2)	1.7(1)	*b*		
monoclinic	220−550	0.97(1)	2.80(4)	6.6E−7	0.93(2)	12.6(2)
hexagonal from monoclinic	460−220	0.92(1)	3.52(5)	2.8E−5		

[a] Read at 7.2 × 10^{-5}. [b] $\sigma_{900°C}$ = 0.47 S cm^{-1}.

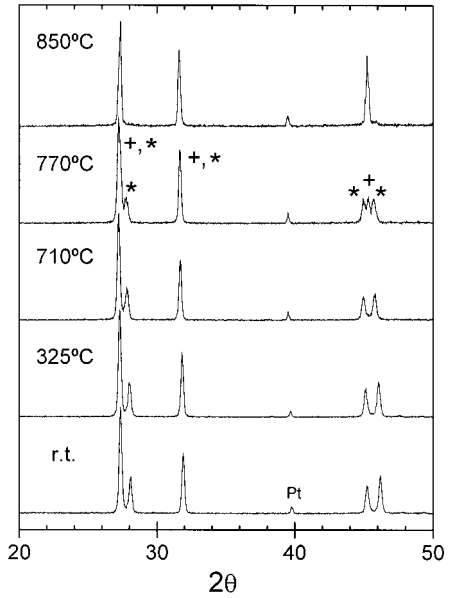

Figure 4. X-ray patterns recorded for hexagonal $Bi_{1.56}U_{0.22}La_{0.22}O_{3.33}$ at the temperatures indicated. (* and + symbols represent hexagonal H and cubic C* polymorphs, respectively).

fects.[18] M'' is related to the impedance through the expression $M''(f) \propto fZ'(f)$, where f and Z' are the frequency and the real impedance, respectively. The frequency dependence of M'' showed, for the three polymorphs, an asymmetric peak that shifted toward higher frequencies at increasing temperatures, in a similar way to that reported for the $Bi_{1.33}U_{0.33}La_{0.33}O_{3.5}$ composition.[9] The plot, not shown here, of the frequency (log f) at the maximum of the M'' peak against inverse temperature (1000/T) showed a straight line that was well-fitted to the expression $f = f_0 \exp(-E_f/kT)$. It was observed that the activation energy E_f for the three polymorphs coincided with the activation energy E_σ deduced from conductivity data (Table 2), evidencing that the impedance arc detected at low temperature is dominated by the grain-interior response, that is, by motion of O^{2-} ions inside the grains.

High-Temperature X-ray Powder Diffraction. X-ray patterns recorded for the hexagonal polymorph at some significant temperatures are presented in Figure 4. The patterns recorded at increasing temperature up to 710 °C show the same profile as the starting hexagonal polymorph, but the maxima are progressively shifted toward lower 2θ angles due to dilatation of the sample. At 770 °C a new maxima at 45.3° 2θ (marked + in the figure) is clearly seen. It corresponds to the

(18) Hodge, I. M.; Ingram, M. D.; West, A. R. *J. Electroanal. Chem.* **1976**, *74*, 125.

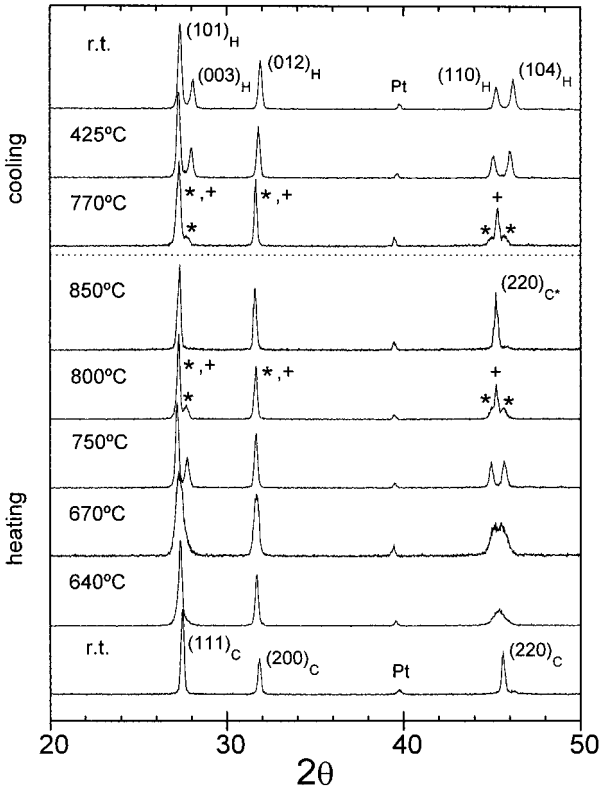

Figure 5. X-ray patterns recorded for cubic $Bi_{1.56}U_{0.22}La_{0.22}O_{3.33}$ at the temperatures indicated. (* and + symbols represent hexagonal H and cubic C* polymorphs, respectively).

$(220)_C$ peak of a new fluorite-type material, which is obtained at 850 °C as a single phase. It will be shown later that this new cubic phase (labeled C*) with cell parameter a_{C*} = 5.6801(3) Å is different from the starting cubic C polymorph. The X-ray patterns recorded on cooling (not shown in Figure 4) are similar to those recorded on heating, indicating reversibility in the structural transformations.

For the cubic polymorph, the patterns recorded at different temperatures are presented in Figure 5. Between room temperature and 640 °C the material remains cubic although sample dilatation causes a shift of the peaks toward lower 2θ angles. From 550 to 640 °C the diffraction maxima broaden, and at 670 °C a splitting of the $(111)_C$ into the $(101)_H$ and $(003)_H$, and the $(220)_C$ into the $(110)_H$ and $(104)_H$, is observed. The new pattern can be fully indexed in a hexagonal lattice with cell parameters a_H = 4.016(2), c_H = 9.727(5) Å, and c_H/a_H = 2.422. On increasing the temperature the splitting goes further, and at 725 °C the pattern corresponds to a hexagonal single phase, the cell parameter being a_H = 4.036(1), c_H = 9.646(4) Å, and

$c_H/a_H = 2.389$. At 800 °C peaks of the hexagonal and the new C* cubic phases are present. Between 800 and 850 °C the intensity of the $(003)_H$, $(110)_H$, and $(104)_H$ peaks diminishes, while that of the $(220)_{C^*}$ peak develops significantly. Finally, at 850 °C the pattern coincides with that obtained for the C* single phase. From these data it can be stated that the starting C cubic polymorph transforms into a hexagonal phase in the interval 640−750 °C, and this latter phase transforms again into the cubic C* phase between 750 and 850 °C. Patterns recorded to 425 °C on cooling are similar to those obtained on heating, but from the latter temperature to room temperature the patterns coincide with that of the starting H polymorph (Figures 4 and 5). The hysteresis of the H → C* transition already observed in the DSC curve (Figure 2b,d) is also noticed (see patterns at 770 and 800 °C in Figure 5).

Patterns recorded for the monoclinic polymorph at the indicated temperatures are shown in Figure 6. The polymorph remains stable below 700 °C. At this temperature weak maxima of the hexagonal polymorph (marked * in the figure) are present. They develop on heating the sample at 700 °C for 4 h, whereas peaks of the starting monoclinic phase vanish progressively. Patterns recorded between 750 and 800 °C show, besides the peaks of the hexagonal phase, new peaks of the cubic C* phase (marked + in the figure), the latter peaks being fully developed with increasing temperature. Finally, at 850 °C the pattern only shows the peaks characteristic of the cubic C* phase, indicating that this phase is obtained as a single phase. The X-ray pattern recorded at room temperature after the cooling run coincides with that of the starting hexagonal polymorph.

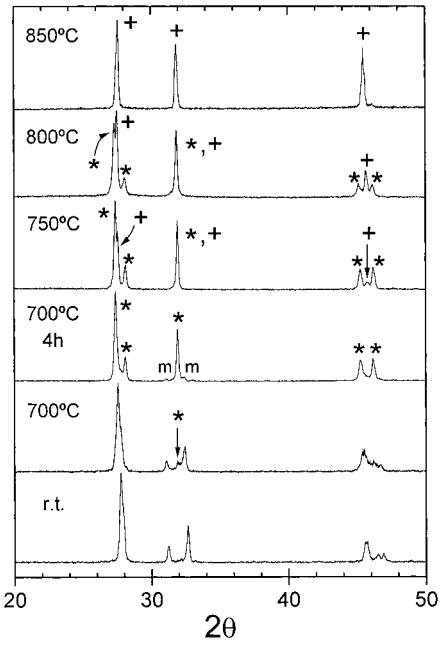

Figure 6. X-ray patterns recorded for monoclinic $Bi_{1.56}U_{0.22}La_{0.22}O_{3.33}$ at the temperatures indicated. (* and + symbols represent hexagonal and cubic polymorphs, respectively; m refers to the monoclinic phase).

Discussion

Figure 7 shows the variation of conductivity (log σ) vs inverse temperature (1000/T) for the hexagonal (○), cubic (□), and monoclinic (△) $Bi_{1.56}U_{0.22}La_{0.22}O_{3.33}$ polymorphs. The comparative study shows that at temperatures below 400 °C the ionic conductivity for the cubic phase is somewhat higher than for the hexagonal one and more than 1 order of magnitude higher than the monoclinic polymorph (Table 2). The latter decrease agrees with the behavior observed in some other bismuth-based oxides in which noncubic phases formed on annealing show lower oxide ion conduction.[3,19−22] Our experimental data for the three polymorphs in the low-temperature region are well fitted to the Arrhenius equation (see the three straight lines in the figure). The value of the activation energy, as calculated from the slope of the straight lines, is close (0.90−0.97 eV) for the three polymorphs. Since the activation energy gives a measure of the hindrance in the movement of the O^{2-} ions, we conclude that it is similar for the three polymorphs. In the high-temperature region (820−950 °C) in which a cubic (C^*) single phase is formed (Figures 4−6) conductivity data follow a common linear dependence. However, the activation energy is significantly smaller (0.47 eV) than that obtained for the cubic C polymorph in the low-temperature region (0.91 eV). This result indicates that the cubic C* phase formed at high temperature is different from the starting cubic C polymorph. Another argument supporting that the starting C cubic and the C* phases are different is based on the fact that the value of the cubic a_{C^*} parameter is larger than expected from the extrapolation at high-temperature of the cell parameter of the C polymorph (see dotted line in Figure 9a).

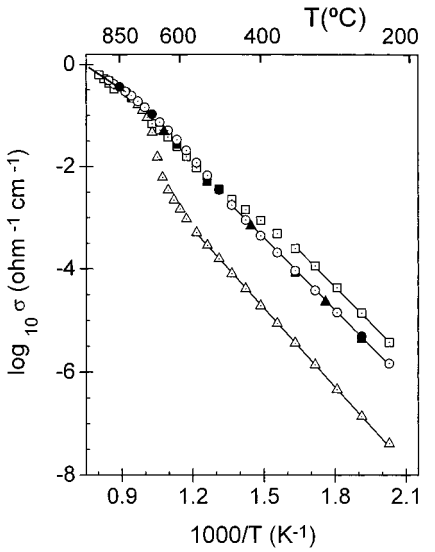

Figure 7. Plot of log σ vs 1000/T for the hexagonal (○), cubic (□), and monoclinic (△) $Bi_{1.56}U_{0.22}La_{0.22}O_{3.33}$ polymorphs. Open and closed symbols stand for the heating and cooling runs, respectively.

Besides the linear dependencies observed at low and high temperature in the conductivity plots, there are other intermediate curved regions that do not follow an

(19) Fung, K. Z.; Baek, H. D.; Virkar, A. V. *Solid State Ionics* **1992**, *52*, 199.
(20) Jiang, N.; Buchanam, R. M.; Henn, F. E. G.; Marshall, A. F.; Stevenson, D. A.; Wachsman, E. D. *Mater. Res. Bull.* **1994**, *29*, 247.
(21) Jiang, N.; Buchanam, R. M.; Stevenson, D. A.; Nix, W. D.; Li, J. Z.; Yang, J. L. *Mater. Lett.* **1995**, *22*, 215.
(22) Su, P. Virkar, A. V. *J. Am. Ceram. Soc.* **1996**, *79*, 371.

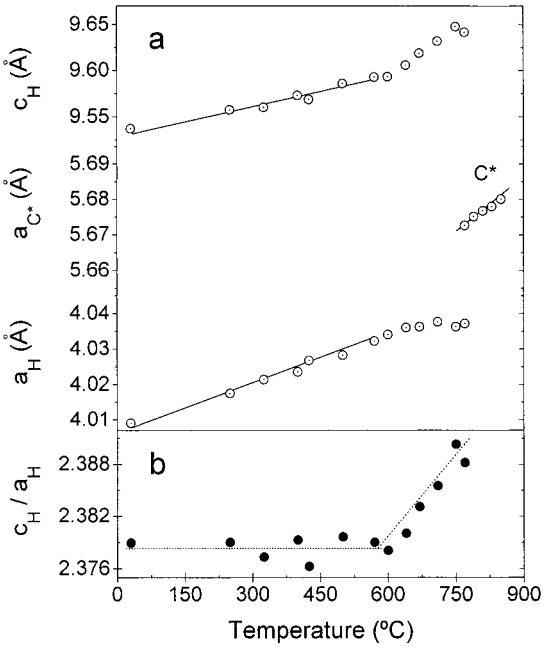

Figure 8. Evolution with temperature of (a) lattice parameters of the starting hexagonal (c_H, a_H) and of the cubic (a_{C^*}) polymorphs formed on heating and (b) c_H/a_H ratio.

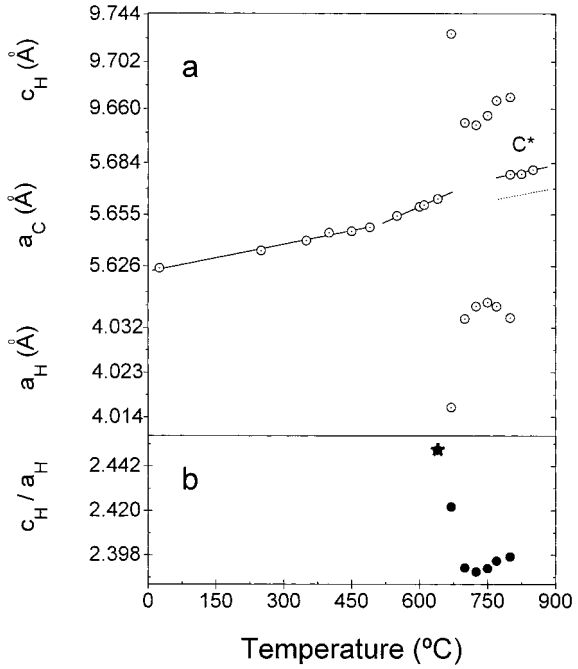

Figure 9. Evolution with temperature of (a) lattice parameters of the starting cubic (a_C), hexagonal (c_H, a_H), and cubic (a_{C^*}) polymorphs formed on heating and (b) c_H/a_H ratio (calculated $c_H/a_H = 2.45$ for a fcc phase marked *).

Arrhenius behavior. They are detected in the following temperature intervals: one in the range 490−790 °C for the hexagonal polymorph, two in the ranges 310−520 and 550−790 °C for the cubic polymorph, and another one between 550 and 790 °C for the monoclinic polymorph (Figure 7). The existence of non-Arrhenius dependencies has also been reported for several Bi_2O_3-based electrolytes[1,23−25] and other oxide ion conductors.[26,27] However, only a few studies have been done to explain this behavior.[28,29] To understand the cause of this phenomenon, we have carefully analyzed the high-temperature X-ray powder diffraction patterns of the three polymorphs. Plots of the cell parameters vs temperature for the starting hexagonal and cubic polymorphs, as well as for the intermediate phases formed on heating are shown in Figures 8a and 9a, respectively. In Figures 8b and 9b the variation of c_H/a_H ratio for the hexagonal phases is also presented.

For the hexagonal polymorph c_H and a_H increase linearly between room temperature and 570 °C due to dilatation while the c_H/a_H ratio remains almost constant. However, between 570 and 770 °C the cell parameters depart from the linear dependence, c_H increasing faster and a_H reaching a plateau (Figure 8a). The c_H/a_H ratio sharply increases from 2.379 at 570 °C to 2.388 at 770 °C (Figure 8b), indicating that in addition to dilatation the hexagonal polymorph is undergoing a structural modification. It is worth mentioning that a simple operation transforms a cubic face-centered cell into a hexagonal cell:[12,30,31] $a_H = a_C\sqrt{2}/2$, $c_H = a_C\sqrt{3}$. In this hexagonal description, the calculated c_H/a_H ratio for a fcc cell is 2.45. Departures from this particular value can be taken as a measure of the hexagonal distortion of a fcc cell. Having in mind these structural relationships, the observed increase of the c_H/a_H ratio indicates that between 570 and 750 °C the hexagonal polymorph becomes less and less anisotropic going toward a cubic phase. Between 750 °C ≤ T < 790 °C, the H and C* phases coexists, and above 850 °C the C* is obtained as a single phase. Therefore, the bend region observed in the conductivity plot (○ in Figure 7) between 490 and 790 °C is due (i) to the continuous structural modification of the hexagonal polymorph and (ii) to the coexistence of the modified hexagonal polymorph and the C* phase which develops at expenses of the former.

For the starting cubic polymorph, the cell parameter increases linearly from room temperature to 490 °C due to sample dilatation, but from 550 to 640 °C the a_C parameter increases faster (Figure 9a), indicating a continuous structural modification of the starting cubic polymorph. Above 670 °C a hexagonal single phase is formed (Figure 5). This phase undergoes a continuous evolution between 670 and 725 °C becoming more hexagonal, as deduced from the decrease of the c_H/a_H ratio. Above 725 °C a slight increase of c_H/a_H is observed, indicating the premonitory change of the hexagonal phase, which is going toward a cubic symmetry. In fact, at 850 °C the cubic C* phase is obtained as a single phase. Between 800 and 850 °C a mixture of the hexagonal and cubic C* is observed. The gradual structural modification undergone by the cubic C phase leading to the H polymorph, the continuous evolution

(23) Takahashi, T.; Esaka, T.; Iwahara, H. *J. Appl. Electrochem.* **1975**, *5*, 197.
(24) Verkerk, J. M.; Burggraaf, A. J. *J. Electrochem. Soc.* **1981**, *128*, 75.
(25) Qiu, L.; Yang, Y. L.; Jacobson, A. J. *J. Mater. Chem.* **1997**, *7*, 249.
(26) Bauerle, J. E.; Hrizo, J. *J. Phys. Chem. Solids* **1969**, *30*, 565.
(27) Kudo, T.; Obayashi, H. J. *Electrochem. Soc.* **1975**, *122*, 142.
(28) Verkerk, M. J.; van de Velde, G. M. H.; Burggraaf, A. J.; Helmholdt, R. B. *J. Phys. Chem. Solids* **1982**, *43*, 1129.
(29) Mercurio, D.; Champarnaud-Mesjard, J. C.; Frit, B.; Conflant, P.; Boivin, J. C.; Vogt, T. *J. Solid State Chem.* **1994**, *112*, 1.
(30) Koster, A. S.; Renaud, J. P. P.; Rieck, G. D. *Acta Crystallogr.* **1975**, *B31*, 127.
(31) Amarilla, J. M.; Rojas, R. M.; Herrero, M. P. *Chem. Mater.* **1995**, *7*, 341.

of the latter, and finally the H → C* phase transition account for the second non-Arrhenius dependence observed at 550−790 °C in the conductivity plot of the cubic C polymorph (□ in Figure 7). For the first curved region (310−520 °C) neither change in symmetry nor irregular variations of the cubic cell parameter have been observed, and up to date we have not been able to provide a reliable explanation for it.

For the monoclinic polymorph the conductivity values smoothly depart from the Arrhenius behavior between 580 and 640 °C (△ in Figure 7). However, from 640 to 720 °C conductivity greatly increases from 3.46×10^{-3} S cm^{-1} at 640 °C to 9.12×10^{-2} S cm^{-1} at 720 °C, and between 720 and 790 °C conductivity data practically coincide with those found for the hexagonal and cubic polymorphs in this temperature range. From high-temperature X-ray diffraction patterns shown in Figure 6, it can be stated that the M → H and H → C* phase transformation takes place between 690 and 800 °C. Therefore, the curvature observed in the conductivity plot of the monoclinic polymorph (△ in Figure 7) is ascribed to the coexistence of the M,H and H,C* phases during the corresponding phase transitions.

In the cooling run the hexagonal sample (closed circles in Figure 7) behaves identical with the heating run showing the same Arrhenius and non-Arrhenius regions already described. The hysteresis of the H → C* transformation observed in DSC and high-temperature X-ray powder diffraction is also noticed. The cubic and monoclinic polymorphs (closed squares and triangles, respectively, in Figure 7) behave differently from heating. They follow the pattern shown by the hexagonal phase, this being the polymorph obtained after the conductivity measurements.

Results indicated above allow us to conclude that the Arrhenius dependencies of conductivity are associated with the presence of single phases, while the non-Arrhenius behaviors are due to structural transformations. These transformations are (i) the continuous structural evolution undergone by the polymorphs, as is specially noticeable for the intermediate hexagonal phase formed on heating the cubic C polymorph, and (ii) the first-order phase transitions, such as the H → C* transformation.

Acknowledgment. Financial support by CICyT (Project MAT95/0899) is acknowledged. Dr. J. M. Amarilla thanks the CSIC for a contract under the mentioned project.

CM970573J